Proton conduction based on intracrystalline chemical reaction

G. Schuck[1,2]**, R.E. Lechner**[1,*]**, K. Langer**[2]

[1] Hahn-Meitner-Institut, Glienicker Strasse 100, 14109 Berlin, Germany
[2] Inst. für Angewandte Geowissenschaften I, Technische Universität Berlin, Ernst-Reuter-Platz 1, 10587 Berlin, Germany

Abstract. Proton conductivity in $M_3H(SeO_4)_2$ crystals (M = K, Rb, Cs) is shown to be due to a dynamic disorder in the form of an intracrystalline chemical equilibrium reaction: alternation between the association of the monomers $[HSeO_4]^{1-}$ and $[SeO_4]^{2-}$ resulting in the dimer $[H(SeO_4)_2]^{3-}$ (H-bond formation) and the dissociation of the latter into the two monomers (H-bond breaking). By a combination of quasielastic neutron scattering and FTIR spectroscopy, reaction rates were obtained, as well as rates of proton exchange between selenate ions, leading to diffusion. The results demonstrate that this reaction plays a central role in the mechanism of proton transport in these solid-state protonic conductors.

PACS: 78.70.Nx; 66.10.Ed; 25.40.Fq; 25.70 Bc; 28.20.Cz; 61.12.Ex

The crystalline compounds with the general formula $M_3H(XO_4)_2$, (M = K, Rb, Cs; X = S, Se), where hydrogen bonding plays an important role, have high- temperature phases with rhombohedral symmetry and extremely high protonic conductivity, i.e. they are solid-state protonic conductors (SSPC). The crystallographic phases existing at lower temperatures are monoclinic or triclinic and show lower, but still appreciable protonic conductivities in a fairly broad temperature range in the vicinity of the SSPC phase transition [1, 2]. The diffusive proton motion relevant to the protonic conductivity is accessible to quasielastic incoherent neutron scattering (QINS) techniques [3, 4].

We have obtained such information from a series of QINS studies on several solid-state protonic conductor materials with layered pseudo-hexagonal structures, namely $CsOH \cdot H_2O$ (see [4]), β-$Zr(HPO_4)_2$ [5] and $Rb_3H(SeO_4)_2$ [6].

In the present paper we report on results from experiments on $Rb_3H(SeO_4)_2$, using medium-resolution QINS and FTIR spectroscopy.

*Corresponding author.
(Fax: +49-30/8062-2181, E-mail: lechner@hmi.de)

1 Structure and SSPC phase transition

The time-averaged crystal structure of $Rb_3H(SeO_4)_2$ [7–10] can be described as a sequence of Rb$\cdots$H[SeO$_4$]$_2$ – layers alternating with Rb- coordination polyhedra layers, both perpendicular to the pseudo-hexagonal c-axis. The rubidium atoms in the Rb-layers, of type Rb(2), have 9-fold coordination by the oxygen atoms forming the bases (O(1), O(3) and O(4)) of the selenate tetrahedra, which are parallel to the layers. The top oxygen atoms (O(2)) of the selenate tetrahedra are connected by hydrogen bonds with each-other, forming $H[SeO_4]_2^{3-}$ dimers at low temperatures ("zero-dimensional" H-bond network; see Fig. 1a) and layers of two-dimensional dynamically disordered H-bond networks in the proton conducting high-temperature phase ($T > 449$ K; Fig. 1b). The time averaged structure of the latter is trigonal, space group ($R\bar{3}m$).

2 QINS: the 'trigonal asymmetric H-bond' (TAHB) model

In the QINS measurements, we have directly observed translational proton diffusion occurring on the 10^{-8} s time scale [11], as well as much faster localized diffusive proton motions (time scales: 10^{-9} s to 10^{-11} s; spectrometer NEAT [5]). Only the latter will be discussed here. A careful EISF study [6, 12] suggests that the local proton-density distribution resulting from a limited time-averaging (from 10^{-11} s to 10^{-10} s) already has threefold symmetry, and that it comprises the regions of the three H-bonds connecting a given (selenate top) oxygen to its three neighbouring selenate top oxygens in the same proton conducting plane. The "trigonal-asymmetric hydrogen bond" model [12] corresponds to this picture: The local proton site arrangement comprises a central site 1, with an average proton residence time τ_1, connected to 3 external sites with identical residence times τ_2 by the jump vectors R_{21}, R_{31} and R_{41}. The 3 vectors (of equal lengths) point into the directions of the three

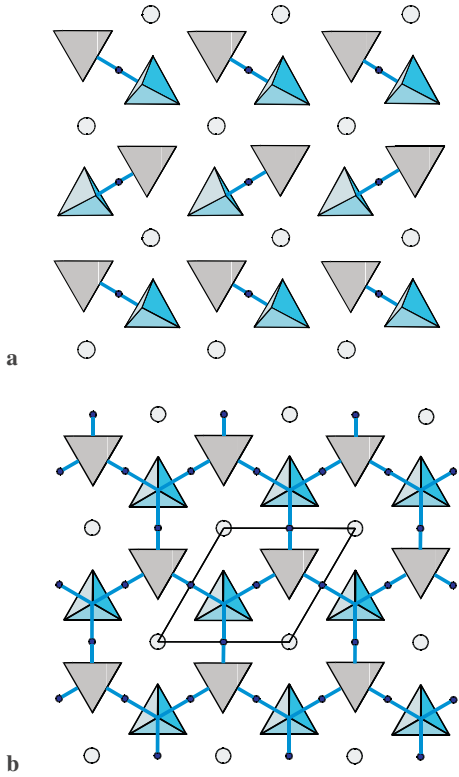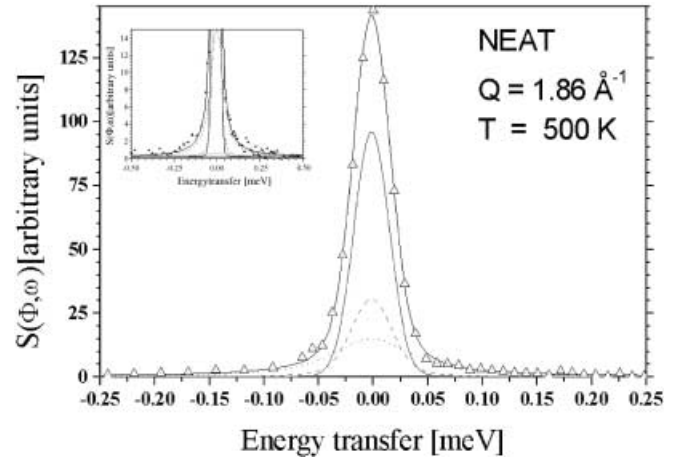**Fig. 2.** Fit of the TAHB model to a spectrum measured at 500 K (NEAT; elastic resolution FWHM $= 34\,\mu$eV; $Q = 1.86\,\text{Å}^{-1}$)

Fig. 1. a Monoclinic $Rb_3H(SeO_4)_2$: "zero-dimensional" H-bond network as seen in a projection along the *c*-axis. *Small circles*: protons; *large circles*: Rb^+ ions; **b** Trigonal $Rb_3H(SeO_4)_2$: two-dimensional dynamically disordered H-bond network in plane perpendicular to *c*-axis

H-bonds (Fig. 1b), with end points located fairly close to the bond centers. The two jump rates, $1/\tau_1$ and $1/\tau_2$, are allowed to be different from each-other, implying an asymmetry of the potential in which the proton is moving, on the time-scale of this experiment. The time-dependent site occupation probabilities for the 4 sites are denoted by $W_j(t)$. Their time-averages,

$$W_j^\infty = \lim_{t\to\infty} W_j(t)\,, \tag{1}$$

can be used to introduce an order parameter η,

$$\eta = 2W_1^\infty - 1\,, \tag{2}$$

where full order ($\eta = 1$) means no proton exchange with the external sites. The incoherent scattering function of the model is given by [12]:

$$S_S(\boldsymbol{Q}, \omega) = \text{EISF}(\boldsymbol{Q})\delta(\omega) + \text{QISF}_2(\boldsymbol{Q})L_2(H_2, \omega)$$
$$+ \text{QISF}_3(\boldsymbol{Q})L_3(H_3, \omega)\,. \tag{A18}$$

Here the elastic and quasielastic incoherent structure factors, EISF and QISF_j, depend on the jump vectors and on η. The two Lorentzians are given by:

$$L_j(H_j, \omega) = H_j/\left[\left(H_j\right)^2 + \omega^2\right]/\pi\,, \tag{3}$$
$$H_2 = (3/\tau_1 + 1/\tau_2) = 6/\left(1 - \eta\right)/\tau_1\,, \tag{4}$$
$$H_3 = 1/\tau_2 = 3\left(1 + \eta\right)/\left(1 - \eta\right)/\tau_1\,. \tag{5}$$

A comparison of this model to the QINS spectra obtained at 500 K (Fig. 2) gave $\eta = 0.746$ and $R_{21} = 1.785\,\text{Å}$. The asymmetry represented by this value of η is appreciable. Accordingly, the occupancy of site 1 is at least 5 times larger than the sum of the occupation probabilities of the 3 external sites. From this it also follows, that – at the temperature of the experiment – the average life-time of the dimer is about 20 times shorter than that of the monomers, a consequence of the asymmetry of the potential. The meaning of these observations was discussed in more detail in [6] and [12]. Briefly, the important aspect of the obtained η-value is the result, that the proton essentially remains bonded to the original selenate top oxygen, i.e. to one selenate group, for a period of the order of at least 10^{-10} s. The value of the jump distance R_{21} may however be taken as an indication, that the proton is also exploring – on the 10^{-11} s to 10^{-10} s time scale – a path into the hydrogen bridge, although with rather low probability. We have interpreted these observations as the consequence of the presence of an intracrystalline chemical equilibrium reaction: alternation between the association of the monomers $[HSeO_4]^{1-}$ and $[SeO_4]^{2-}$, resulting in the dimer $[H(SeO_4)_2]^{3-}$ (H-bond formation) and the dissociation of the latter into the two monomers (H-bond breaking) [6].

Reaction rates and potential barriers for association and dissociation processes have been determined, as well as temperature-dependent proton exchange rates between neighbouring selenate ions. A detailed account of these results must however be postponed to a later publication [13].

3 FTIR: vibrational modes of selenate ions

The analysis of the structural properties of the H-bond network in $Rb_3H(SeO_4)_2$ naturally starts from the centro-symmetric monoclinic ($C2/c$) and trigonal ($R\overline{3}m$) crystal structures postulated on the basis of the crystallographic results [7–10]. Our FTIR measurements and factorgroup analysis made however clear, what retrospectively seems obvious: the centro-symmetric (time-averaged) structures are not sufficient for the description of the time-dependent short-range order of the protons. The spectroscopic analysis
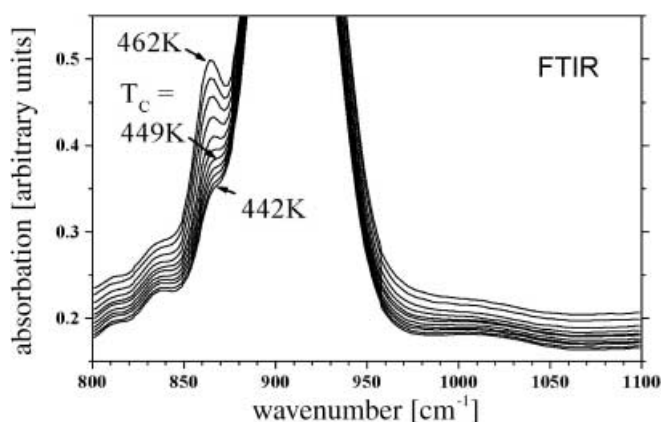
Fig. 3. The ν_1-H[SeO$_4$]$^{1-}$ monomer vibration near 860 cm^{-1}: T-dependence across the SSPC phase-transition

points at the existence of a dynamic proton – "superstructure". This is consistent with the fact that the static model of a "zero-dimensional" H-bond network with centro-symmetric H[SeO$_4$]$_2^{3-}$ dimers attributed to the monoclinic phase, can not explain the observation of a relatively high protonic conductivity in the latter. Factorgroup analysis on the basis of non-centrosymmetric space group symmetries however, leads to a normal mode classification for the crystal, allowing the explicit attribution of specific vibrational symmetry types to the [HSeO$_4$]$^{1-}$ and [SeO$_4$]$^{2-}$ monomers. We have succeeded in identifying such internal modes in the spectra obtained with the FTIR-MS technique using small single crystals in transmission.

The modes were classified in two groups differing by the strength of the monomer coupling. These modes show an interesting temperature dependence in the neighbourhood of the SSPC phase transition (449 K). While the intensities of weakly coupled monomers increase with temperature, those of strongly coupled (i.e. dimer forming) monomers decrease [13]. As an example Fig. 3 shows the temperature behaviour of the ν_1-H[SeO$_4$]$^{1-}$ monomer vibration at 860 cm^{-1}, which corresponds to the weak-coupling case. In agreement with the QINS result, we have interpreted this observation as a manifestation of the chemical equilibrium described above. The T-dependence of the selenate vibrational modes can be understood as due to a variation of the monomer concentration, when the SSPC phase transition is approached from below and consequently the reaction equilibrium is shifted towards the weak-coupling side.

4 Conclusion

We have shown, that the dynamical disorder existing in the high-temperature phase of Rb$_3$H(SeO$_4$)$_2$ can be described by a chemical equilibrium reaction consisting in an alternation between the association of the two monomers [HSeO$_4$]$^{1-}$ and [SeO$_4$]$^{2-}$ resulting in the dimer [H(SeO$_4$)$_2$]$^{3-}$ (formation of a hydrogen bond), and the dissociation of the latter into the two monomers (rupture of the H-bond). The two distinct transient chemical states play different specific roles in the mechanism of protonic conductivity. While in the monomer state the protonated monomer via reorientation makes the proton available for three different elongated (and therefore weak) hydrogen bonds, the dimer state corresponding to the creation of a strong (but short-lived) H-bond, with the proton close to the center of the bond, provides the opportunity for proton transfer across the hydrogen bridge.

References

1. A.I. Baranov, I.P. Makarova, L.A. Muradyan, A.V. Tregubchenko, L.A. Shuvalov, V.I. Simonov: Sov. Phys. Crystallogr. **32**(3), 400 (1987, 1988 AIP)
2. A. Pawlowski, Cz. Pawlaczyk: Ferroelectrics **81**, 201 (1988)
3. R.E. Lechner: Solid State Ionics **61**, 3 (1993)
4. R.E. Lechner: Ferroelectrics **167**, 83 (1995)
5. R.E. Lechner, R. Melzer, J. Fitter: Physica B **226**, 86 (1996)
6. R.E. Lechner, G. Schuck, K. Langer: J. Phys. Soc. Japan **70**, 274 (2001)
7. I.P. Makarova, I.A. Verin, N.M. Shchagina: Sov. Phys. Crystallogr. **31**, 105 (1986)
8. A. Bohn, R. Melzer, R. Sonntag, R.E. Lechner, G. Schuck, K. Langer: Solid State Ionics **77**, 111 (1995)
9. R. Melzer, R. Sonntag, K.S. Knight: Acta. Cryst. C **52**, 1061 (1996)
10. R. Melzer, T. Wessels, M. Reehuis: Solid State Ionics **92**, 119 (1996)
11. R.E. Lechner, G. Schuck, K. Langer, Th. Dippel, W. Renz, M. Casciola: Solid State Ionics, to be publ.
12. R.E. Lechner: Solid State Ionics **145**, 167 (2001)
13. G. Schuck, R.E. Lechner, K. Langer: to be publ.